J|A|C|S
COMMUNICATIONS

Published on Web 08/12/2006

Controlling Carbon Surface Chemistry by Alloying: Carbon Tolerant Reforming Catalyst

Eranda Nikolla, Adam Holewinski, Johannes Schwank, and Suljo Linic*

Department of Chemical Engineering, University of Michigan, Ann Arbor, Michigan 48109-2136

Received May 31, 2006; E-mail: linic@umich.edu

Controlling carbon chemistry on metal surfaces is important in the fields of heterogeneous catalysis and nanotechnology. Controlled formation of C−C bonds is instrumental for carbon nanotube synthesis.[1,2] On the other hand, in hydrocarbon steam reforming, the formation of extended carbon deposits such as graphite or nanotubes leads to catalyst poisoning.[3,4] In this communication we demonstrate that carbon chemistry over metal surfaces can be controlled by alloying. We have employed density functional theory (DFT) calculations along with catalyst synthesis, characterization, and reactor studies to identify a catalyst that is active in hydrocarbon steam reforming and resistant to the formation of carbon deposits.

Steam reforming is a process where a hydrocarbon is converted into hydrogen and oxygenated carbon species. Ni is often used as the catalyst for the reaction.[3] The process is important not only for catalytic hydrogen production but also for direct electrochemical reforming over high-temperature fuel cells.[5,6] It is well established that over Ni catalysts, hydrocarbons decompose into carbon and hydrogen adsorbates.[4,7] Long term stability of the catalyst is governed by its ability to selectively oxidize carbon while preventing C−C bond formation as shown in Scheme 1.

Scheme 1

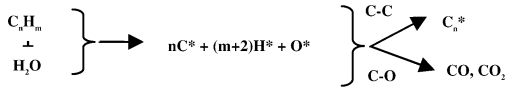

The main problem with Ni is that the rate of C−C bond formation is high, leading to the rapid growth of carbon deposits which poison the catalyst. The catalyst poisoning can be suppressed by increasing the feed steam concentration, which results in higher rates of carbon oxidation and improved stability. However, high steam concentration is not desirable since it lowers the energy density of the products. An optimal catalyst would operate at the steam-to-carbon ratio close to 1 and would preferentially oxidize and desorb carbon rather than form C−C bonds.

It has been established that the formation of carbon deposits on Ni proceeds via C atom diffusion on the catalyst surface and subsequent C−C bond formation at the interface of Ni and carbon nucleation centers.[2,8] We have employed DFT calculations[9b] to study carbon chemistry over Ni and Ni alloys. Our objective was to identify a Ni-containing alloy which, relative to monometallic Ni, favors carbon oxidation over C−C bond formation. Alloy catalysts have previously been utilized in liquid[9,10] and gas-phase reforming of hydrocarbons.[11−15]

Our DFT calculations in Figure 1 show that graphite is the lowest energy state of carbon on the Ni (111) surface. We calculate that the adsorption energy per carbon atom in a graphene sheet on Ni (111) is by ∼1.3 eV more exothermic than the adsorption energy for carbon adsorbed on Ni (111) at $^1/_9$ ML. Clearly, there is a thermodynamic driving force to form sp^2 carbon deposits. Figure 1 shows that the activation barrier for C atom diffusion on Ni (111)

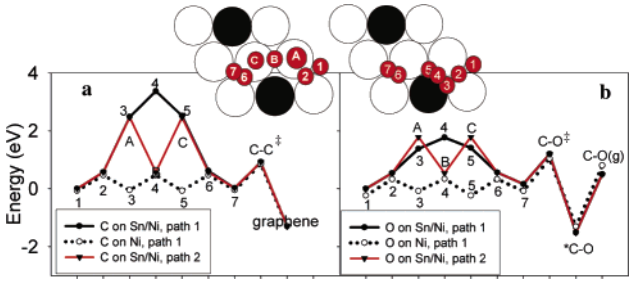

Figure 1. Inserts show the high-symmetry sites along C and O atom (small red circles) diffusion pathways on the (111) surface. The diffusion pathways consist of a C or O atom moving along path 1 (1-2-3-4-5-6-7, left insert) or path 2 (1-2-A-B-C-6-7, right insert). Large dark circles are Sn, large light circles are Ni. Panel a shows the DFT calculated energies for C atom diffusion on pure Ni and Sn/Ni. C−C‡ represents DFT calculated activation energy for C atom attachment to a nucleation site (modeled as graphene sheet, not shown) on Ni.[8] Zero energy corresponds to the C atom adsorbed on Sn/Ni and separated from a nucleation site. Panel b shows the DFT calculated energies for O atom diffusion on Ni and Sn/Ni. The pathway consists of O atom diffusion over the surfaces and subsequent formation of adsorbed CO followed by CO desorption. C−O‡ characterizes DFT calculated activation energy for C−O bond formation on Ni (111). Zero energy corresponds to a C and an O atom separated far apart from each other on the most stable sites of Sn/Ni.

is 0.5 eV, suggesting that C atoms are very mobile on the surface at the reaction temperature of ∼1050 K. The high rate of C atom diffusion along with low activation barrier for C atom attachment to the nucleation center (modeled as a graphene sheet on Ni), calculated to be 0.92 eV,[8] results in rapid formation of extended sp^2 carbon deposits.[16]

Figure 1 demonstrates that on Ni (111) the pathways leading to C-oxidation have comparable overall activation barriers as those resulting in the C atom attachment to the carbon nucleation center. Figure 1 also shows that on a Sn/Ni surface alloy—the surface alloy is characterized by Sn displacing Ni atoms from the top Ni (111) layer—the relative kinetics of C−O and C−C bond formation is significantly different than on Ni. For example, for the configuration in Figure 1, the kinetic barriers for C and O atom diffusion on the Sn/Ni (111) surface are by 1.9 and 1.2 eV larger than the respective kinetic barriers on Ni (111). The dramatic Sn-induced increase in the diffusion barriers suggests that C and O atom diffusion is kinetically important for the respective C−C and C−O bond formation over Sn/Ni and that on the alloy the overall rate of C-oxidation is much greater than that of C−C bond formation. This suggests that the growth of carbon deposits should be suppressed by Sn alloying of Ni.

Furthermore, our DFT calculations show that in the limit of small Sn concentration, the formation energy of Sn/Ni surface alloy is lower than the formation energy of Sn bulk alloys or the formation energy corresponding to pure Sn and Ni phases (see Supporting Information). This is important since it suggests that there exists a thermodynamic driving force to form and sustain a Sn/Ni surface

10.1021/ja0638298 CCC: $33.50

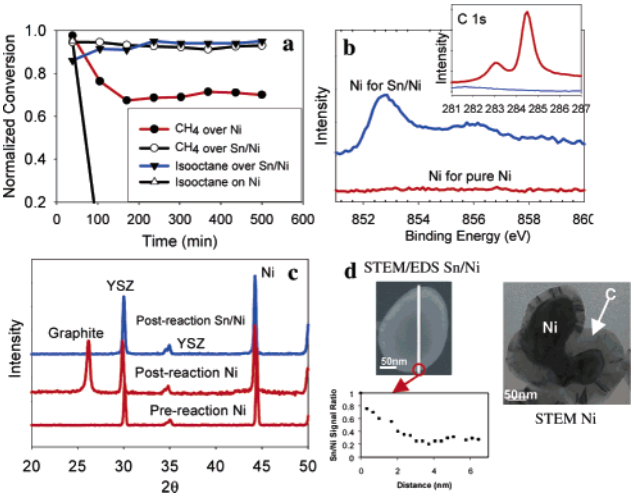

Figure 2. (a) Normalized conversion, calculated as the ratio of measured conversion to the highest conversion of methane and isooctane over Ni/YSZ, is recorded as a function of time on stream. Steam-to-carbon ratio was 0.5 and 1.5 for methane and isooctane, respectively. Panel b shows Ni 2p X-ray photoelectron spectra after isooctane reforming on Ni (red) and on Sn/Ni (blue). Insert shows postreaction carbon (C 1s) spectra for monometallic Ni (red) and Sn/Ni (blue). Panel c is XRD spectra for post-isooctane Ni and Sn/Ni, and for fresh Ni catalysts. Panel d shows the postreaction STEM micrograph of Ni and Sn/Ni. Ni particles are completely covered with carbon deposits while Sn/Ni is carbon-free. Furthermore, elemental mapping of Sn/Ni particles via line scan (STEM/EDS) suggests surface alloying. Lower panel shows that Sn/Ni ratio diminishes as the probe moves from the particle bottom edge upward, indicating the Sn surface enrichment.

alloy. These observations are supported by our experimental results below. We have also calculated that aside from the formation of Sn/Ni surface alloy, there is a favorable thermodynamic driving force for Sn to displace Ni atoms from the step-edge sites. In these configurations the Sn step-edge atoms effectively repel C atoms from the low-coordinated step sites. Since low-coordinated step sites have been proposed to play a role in the nucleation and growth of carbon deposits over Ni,[2,8] this arrangement of Sn atoms further lowers the propensity of the alloy to form carbon deposits.

To test the predictions of the DFT calculations we have synthesized and characterized monometallic Ni and Sn/Ni catalysts with high metal loading (~35 wt %) supported on yttria-stabilized zirconia (YSZ). This preparation procedure resulted in fairly large catalytic particles (0.1−1 μm in diameter). X-ray photoelectron spectroscopy (XPS) demonstrated that the surface of Sn/Ni is enriched with Sn. For example, the Sn concentration in the alloy surface layers, for a sample that contained 1 wt % of Sn with respect to Ni (1% Sn/Ni), was measured with XPS to be ~25%. These measurements justify the model utilized in the DFT calculations. The Sn surface enrichment was further corroborated by scanning transmission electron microscopy with elemental analysis via energy dispersive X-ray spectroscopy (STEM/EDS), shown in Figure 2d.

In Figure 2a we also show the results obtained in catalytic steam reforming of isooctane and methane over pure Ni and 1% Sn/Ni catalysts. The reactor was operated at 1073 K with steam-to-carbon ratios of 0.5 and 1.5 for methane and isooctane, respectively. Figure 2a demonstrates that monometallic Ni rapidly deactivates under these conditions. Unlike Ni, the Sn/Ni catalyst is active and stable for as long as it was kept on stream, approximately 12 h.

Post-isooctane reforming XPS for monometallic Ni, shown in Figure 2b, demonstrates that the catalyst is completely covered by carbon deposits. While the Ni electronic signal was not detected, we observed C 1s signals at 284.5 eV, indicative of sp^2 carbon, and 283.1 eV, which we assign to C atoms in intimate contact with the metal (surface carbide). In post-isooctane reforming XPS analysis of Sn/Ni, Ni $2p_{3/2}$ signal was detected at 253 eV corresponding to metallic Ni, while the C electronic fingerprint was not measured. These results are consistent with the thesis that carbon deposits did not accumulate on Sn/Ni. The results of XPS studies are further supported by postreaction X-ray diffraction (XRD). Figure 2c shows that graphitic carbon is formed over Ni catalyst. On the other hand, the graphite XRD peak was not observed in the postreaction analysis of Sn/Ni. Furthermore, post-reaction micrograph (obtained via STEM) of a Ni particle, Figure 2d, demonstrates that a thick carbon layer forms on the particle. The carbon deposits were not detected in the postreaction STEM studies of the Sn/Ni catalyst.

The reactor and characterization studies presented in Figure 2 illustrate that Sn/Ni catalyst is much more carbon-tolerant than monometallic Ni. We note that we have obtained similar results for other hydrocarbons and for a broad range of operating steam-to-carbon ratios.

In conclusion, we have demonstrated that carbon chemistry on metal surfaces can be manipulated by alloying. Computational chemistry was utilized along with various experimental tools to guide the formulation of novel catalysts based on the understanding of the underlying atomic-scale phenomena that govern the surface chemistry.[17,18]

Acknowledgment. We gratefully acknowledge the support of the U.S. Department of Energy (Grants FG-02-05ER15686 and FC26-05-NT-42516) and the U.S. Army under Cooperative Agreement Number W56HZV-05-2-0001.

Supporting Information Available: Computational and experimental methods. This material is available free of charge via the Internet at http://pubs.acs.org.

References

(1) Ajayan, P. M. *Chem. Rev.* **1999**, *99*, 1787.
(2) Helveg, S.; Lopez-Cartes, C.; Sehested, J.; Hansen, P. L.; Clausen, B. S.; Rostrup-Nielsen, J. R.; Abild-Pedersen, F.; Norskov, J. K. *Nature* **2004**, *427*, 426.
(3) Rostrup-Nielsen, J. R. Catalytic Steam Reforming. In *Catalysis − Science and Technology*; Springer: Berlin, 1984; Vol. 5.
(4) Bengaard, H. S.; Norskov, J. K.; Sehested, J.; Clausen, B. S.; Nielsen, L. P.; Molenbroek, A. M.; Rostrup-Nielsen, J. R. *J. Catal.* **2002**, *209*, 365.
(5) Atkinson, A.; Barnett, S.; Gorte, R. J.; Irvine, J. T. S.; Mcevoy, A. J.; Mogensen, M.; Singhal, S. C.; Vohs, J. *Nat. Mater.* **2004**, *3*, 17.
(6) Rostrup-Nielsen, J. R.; Christiansen, L. J. *Appl. Catal., A.* **1995**, *126*, 381.
(7) Abild-Pedersen, F.; Lytken, O.; Engbaek, J.; Nielsen, G.; Chorkendorff, I.; Norskov, J. K. *Surf. Sci.* **2005**, *590*, 127.
(8) Abild-Pedersen, F.; Norskov, J. K.; Rostrup-Nielsen, J. R.; Sehested, J.; Helveg, S. *Phys. Rev. B.* **2006**, *73*.
(9) (a) Shabaker, J. W.; Huber, G. W.; Dumesic, J. A. *J. Catal.* **2004**, *222*, 180. (b) Laursen, S.; Linic, S. *Phys. Rev. Lett.* **2006**, *97*, 026101.
(10) Shabaker, J. W.; Simonetti, D. A.; Cortright, R. D.; Dumesic, J. A. *J. Catal.* **2005**, *231*, 67.
(11) Nichio, N.; Casella, M. L.; Santori, G. F.; Ponzi, E. N.; Ferretti, O. A. *Catal. Today* **2000**, *62*, 231.
(12) Hou, Z. Y.; Yokota, O.; Tanaka, T.; Yashima, T. *Appl. Surf. Sci.* **2004**, *233*, 58.
(13) Padeste, C.; Trimm, D. L.; Lamb, R. N. *Catal. Lett.* **1993**, *17*, 333.
(14) Trimm, D. L. *Catal. Today* **1999**, *49*, 3.
(15) Wang, L. S.; Murata, K.; Inaba, M. J. *J. Power Sources* **2005**, *145*, 707.
(16) We note that we have also studied C atom bulk diffusion and concluded that kinetic activation barriers are very high.
(17) Linic, S.; Barteau, M. A. *J. Am. Chem. Soc.* **2003**, *125* (14), 4034.
(18) Linic, S.; Barteau, M. A. *J. Catal.* **2004**, *224*, 489.

JA0638298